A Computational Investigation of Organic Dyes for Dye-Sensitized Solar Cells: Benchmark, Strategies, and Open Issues

ARTICLE *in* THE JOURNAL OF PHYSICAL CHEMISTRY C · APRIL 2010

Impact Factor: 4.77 · DOI: 10.1021/jp100713r · Source: OAI

3 AUTHORS, INCLUDING:

Filippo De Angelis
Università degli Studi di Perugia
264 PUBLICATIONS **11,206** CITATIONS

A Computational Investigation of Organic Dyes for Dye-Sensitized Solar Cells: Benchmark, Strategies, and Open Issues

Mariachiara Pastore,*,†,‡ Edoardo Mosconi,†,§ Filippo De Angelis,*,† and Michael Grätzel‖

Istituto CNR di Scienze e Tecnologie Molecolari c/o Dipartimento di Chimica, Università di Perugia, via Elce di Sotto 8, I-06123, Perugia, Italy, Istituto Superiore Universitario di Formazione Interdisciplinare Sez. Nanoscienze, Università del Salento Distretto Tecnologico, Via Arnesano 16, 73100 Lecce, Italy, Dipartimento di Chimica, Università degli Studi di Perugia, Via Elce di Sotto, 8 I-06123, Perugia, Italy, and Laboratory for Photonics and Interfaces, School of Basic Sciences, Swiss Federal Institute of Technology, Lausanne, CH-1015, Switzerland

Received: January 25, 2010; Revised Manuscript Received: March 15, 2010

A comprehensive theoretical study on the electronic absorption spectra of a representative group of organic dyes (L0, D4, D5, C217, and JK2) employed in dye-sensitized solar cell devices is reported. A benchmark evaluation on different time-dependent density functional theory (TDDFT) approaches with respect to high-level correlated coupled cluster (CC) and multireference perturbation theory (MRPT) benchmark calculations is performed in the gas phase. The benchmark results indicate that TDDFT calculations using the hybrid MPW1K and the long-range correct CAM-B3LYP functionals represent a valuable tool of comparable accuracy to that of the much more computationally demanding ab initio methods. Thus, the problem of the comparison between the calculated excitation energies and the measured absorption maximum wavelengths has been addressed employing the MPW1K functional and including the solvation effects by a polarizable continuum model. The present results show that taking into account the chemical and physical phenomena occurring in solution (i.e., protonation/deprotonation of the carboxylic function and the explicit solute−solvent interactions) is of crucial importance for a meaningful comparison between the calculated and the experimental absorption spectra. Our investigation paves the way to the reliable computational design and predictive screening of organic dye sensitizers, even before their synthesis, in analogy to what has been achieved for transition-metal complexes.

1. Introduction

A considerable amount of attention and extensive research efforts have been devoted over the last years to dye-sensitized solar cells (DSSCs)[1] as valuable and low-cost alternatives to silicon and other inorganic semiconductor-based photovoltaic devices. Up to now, the renowned N3 and N719 Ru(II)−polypyridyl photosensitizers have shown the highest performances, with solar energy-to-electricity conversion efficiencies exceeding 11%.[2,3] More recently, the possibility of using fully organic dyes have attracted growing interest due to their easily tunable optical properties, higher extinction coefficients, and, above all, low-cost preparation processes with respect to the ruthenium sensitizers. The performances of these metal-free dyes are, however, still lower than those of Ru(II) complexes, with top efficiencies ranging from 9.5%, in the case of the indoline D149 dye,[4,5] to 9.8% for the record C217 dye.[6]

One of the most successful typologies of organic dyes is constituted by the push−pull architecture, based on a dipolar D−π−A structure: the donor group (D) is an electron-rich unit, linked through a π bridge spacer to the electron-acceptor group (A). The A moiety is directly connected to the semiconductor surface, usually trough a carboxylic or cyanoacrylic function. The key factors influencing the efficient injection of the photoexcited electron into the TiO_2 conduction band are the electron conjugation across the linker between the light-harvesting unit and electron-acceptor group, the excited state redox potential, which should be higher than the energy of the conduction band edge of the oxide, and the peculiar charge-transfer (CT) character of the lowest excited state, which should efficiently direct the electron flow from the donor unit toward the semiconductor surface. Although a great variety of combinations among donor, linker, and acceptor units can be found in the recent literature, the dyes showing the highest conversion efficiencies, such as, for instance, JK2[7] and D149,[8] are made up by thriphenilamine or indoline units as D, by rhodanine or cyanoacrylic moieties as A, and by conjugated heteroaromatic rings, mainly thiophene, as linkers (see Figure 1).

Large-scale quantum mechanical calculations, able to accurately predict the electronic and spectroscopic properties of the dyes, would be an extremely powerful and comparably low-cost tool in the beforehand design of new and highly efficient sensitizers. For the most efficient metal-based dyes, the state-of-the art computational methodologies based on density functional theory (DFT) and time-dependent density functional theory (TDDFT) provide accurate results and reproduces well the optical properties of various Ru(II) complexes,[9−12] along with their ground- and excited-state oxidation potentials, allowing us to predict and screen, in some cases, novel synthetic approaches.[13]

For push−pull organic dyes, on the other hand, the reliable calculation of excitation energies still represents an open issue, as a definite and effective computational approach has not yet

* To whom correspondence should be addressed. E-mail: chiara@thch.unipg.it (M.P.), filippo@thch.unipg.it (F.D.A.).
† Istituto CNR di Scienze e Tecnologie Molecolari, Perugia.
‡ Università del Salento Distretto Tecnologico.
§ Dipartimento di Chimica, Università degli Studi di Perugia.
‖ Swiss Federal Institute of Technology.

10.1021/jp100713r
Published on Web 03/29/2010

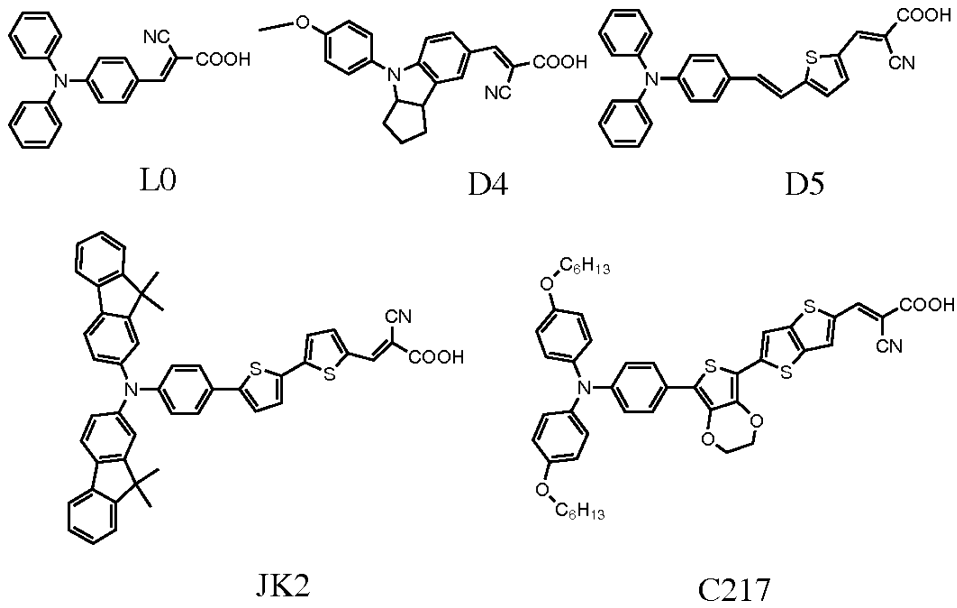

Figure 1. Molecular structures of the L0, D4, D5, JK2, and C217 dye sensitizers.

been defined.[14] As a matter of fact, although TDDFT employing conventional exchange-correlation (x-c) functionals yields quite accurate valence excitation energies both for organic and for inorganic molecules,[9–12,15,16] large underestimations are obtained for excited states with a significant long-range CT character and in the case of molecules with spatially extended π systems.[17–19] This failure has been interpreted as due to the incorrect (faster) long-range decay of standard local x-c functionals and can be also intuitively understood considering the nonlocal nature of the electrostatic interaction involved in a CT state.[17] The use of hybrid functionals, which incorporate a given fraction of nonlocal Hartree−Fock (HF) exchange, partially corrects the wrong asymptotic behavior, but as widely discussed by Magyar and Tretiak,[20] this is a practical strategy rather than an actual solution because the choice of the hybrid functional (i.e., the extent of the HF exchange) is not unique and, as previously shown,[19] is strongly system-dependent. Alternative methodological approaches are grounded on the idea to incorporate an increasing fraction of HF exchange as the interelectronic separation increases; the long-range corrected (LC) functionals by Hirao and co-workers[21–23] and the Coulomb-attenuating B3LYP (CAM-B3LYP) method proposed by Yanai et al.[24] belong to this family of range-separated functionals. Nevertheless, also these long-range corrected techniques suffer from some practical limitations, essentially related to the choice of the range-separation parameter, μ, which, although has been found for CT states to be optimal in the range of 0.2−0.4 a_0^{-1},[21,23,25] turns out to be system- and property-dependent.[26,27]

From a different perspective, the considerably large size of the most efficient organic dyes (∼100 atoms) and the need of taking into account the interactions with the environment for a meaningful comparison with the experimental data rule out the possibility of using high-level correlated wave function-based methods, such as multireference configuration interaction (MR-CI)[28] and multireference perturbation theories (MRPTs)[29,30] or high-order linear response (LR) or equation-of-motion (EOM) coupled cluster,[31] thus making the TDDFT approach the only valuable choice. We notice that a promising alternative methodology, termed SOS-CIS(D), has been recently proposed and successfully applied to charge-transfer excitations of large organic molecules by Rhee and Head-Gordon.[32]

In light of the limitations of TDDFT exposed above and motivated by the huge interest in the computational design and screening of new organic dyes, in this paper, we explore the performance of various TDDFT approaches against high-level correlated benchmark calculations for a significant fraction of organic dyes experimentally employed in DSSC devices. Our aim is to set up a computational approach able to accurately and reliably predict the spectroscopic properties of new (still to be synthesized) organic dyes.

Our investigation is addressed to three systems having triphenylamine-like and cyanoacrylic units as donor and acceptor moieties, selected among the highest-efficiency dyes synthesized so far, namely, the so-termed D5,[33,34] JK2,[7] and C217.[6] Moreover, as the large size of the above-mentioned dyes precludes the possibility to carry out highly correlated ab initio calculations, for benchmarking and calibration purposes, we have selected two additional realistic dyes of smaller size, L0[35,36] and the dye 4 in ref 37 (hereafter termed D4), containing the cyanocrylic unit and, respectively, triphenylamine and indoline donor moieties. The molecular structures of the five investigated dyes are displayed in Figure 1.

2. Methods and Computational Details

2.1. DFT/TDDFT Calculations. The ground-state geometries of both the protonated and the deprotonated dyes have been optimized in the gas phase by DFT with the Gaussian03 package,[38] using the hybrid B3LYP[39] functional and the standard 6-31G* basis set. The impact of the geometry optimization level on the excitation energies was also checked, by carrying out additional geometry optimizations on L0 and D5, using the MPW1K[40] and PBE0[41] x-c DFT functionals and the ab initio MP2 method.

As we shall discuss later, based on some benchmark calculations with the 6-31+G* basis set on L0 and D5, the basis set dimensions[42] and the addition of diffuse functions have negligible effects on the electron density and hence on the accuracy of the DFT and TDDFT results, with differences in the excitation energies never exceeding 0.1 eV. For the TDDFT calculations, performed on the B3LYP optimized ground-state geometries, three different x-c functionals have been used: the two hybrid B3LYP and MPW1K[40] functionals, including 20% and 42% of

Hartree−Fock (HF) exchange, respectively, and the Coulomb-attenuating B3LYP (CAM-B3LYP) approach[24] with the default values of the α, β, and μ parameters (0.19, 0.46, and 0.33, respectively) as implemented in DALTON.[43] Solvation and deprotonation effects were investigated performing TDDFT calculations in various solvents with the nonequilibrium version of the C-PCM model[44] implemented in Gaussian03.[38] This approach does not only correct for solvation effects on the ground-state molecular orbitals and their energies but also includes two-electron terms due to the solvent response to the perturbed density.

2.2. Wave Function-Based Calculations. Here, we shall shortly introduce the basic theoretical concepts and the computational details of the wave function-based methods used in this study: the single- and double-coupled cluster (CCSD) method, its approximate variant (CC2),[45] and the second-order *n*-electron valence state perturbation theory (NEVPT2).[30]

The CCSD method includes all the single and double excitations to infinite order generated from the reference HF wave function, and the CCSD energy is correct to third order. The contribution of single excitations is particularly important for molecular property calculations because it gives an approximate description of orbital relaxation effects. The CC2[45] method was thought as an approximation to CCSD, where the singles equations are left unchanged and the doubles are approximated to the first order with the singles retained as zero-order parameters. The resulting energy is corrected to the second order (a quality comparable to the MP2 energy) with a more favorable scaling with the number of orbitals compared to CCSD.

The equation-of-motion (EOM) CCSD calculations on L0 were carried out with the MOLPRO package[46] adopting the cc-pVDZ basis set by Dunning.[47] The same basis set has also been used for the CC2 calculations, carried out with the TURBOMOLE program,[48] where the method is efficiently implemented exploiting the resolution-of-the-identity (RI) approximation for the bielectronic integrals;[49,50] for the smaller L0, D4, and D5 dyes, RI-CC2 calculation with the larger cc-pVTZ basis was also carried out.

The *n*-electron valence state perturbation theory (NEVPT) is a form of multireference perturbation theory (MRPT) based upon a complete-active space self-consistent field (CASSCF) wave function. Referring the interested reader to a recent review for more details on the method,[30] here, we just highlight that the most appealing property of the NEVPT technique, with respect to other MRPT approaches,[29] is the complete absence of intruder states (i.e., divergences in the perturbative summations), which usually affect the excited state calculations of large systems, especially when reduced active spaces have to be used. Although two variants of NEVPT2 have been formulated and implemented, here, we shall only report and discuss the results obtained with the more accurate "partially contracted" formalism (PC-NEVPT2).[30]

For the definition of the zero-order wave functions of the ground- and of the first-excited state, state-averaged CASSCF (SA-CASSCF) calculations were performed, averaging over the two considered states. Various active spaces in the following, indicated with the (*n*/*m*) notation, where, as usual, *n* and *m* indicate the numbers of active electrons and orbitals, respectively, have been tested. The calculations were performed with the MOLPRO package[46] using the standard 6-31G* basis set, which has already proved to be an optimal compromise between accuracy and computational cost for such large aromatic molecules.[30] For all the coupled cluster and NEVPT2 benchmark calculations, the ground-state geometry of the protonated species optimized in the gas phase at the B3LYP/6-31G* level has been used and the frozen core approximation has been adopted.

TABLE 1: Experimental Absorption Maxima of D4, L0, D5, C217, and JK2

dye	solvent	λ_{max} (nm)	E_{exc} (eV)
D4	ethanol[37]	390	3.18
L0	ethanol[35]	386	3.21
	acetonitrile (deprotonated)[36]	373	3.32
D5	ethanol[34]	441	2.81
	methanol[33]	444	2.79
	methanol + acid (protonated)[33]	474	2.62
	acetonitrile (deprotonated)[36]	427	2.90
C217	chloroform[6]	551	2.25
JK2	ethanol[7]	436	2.84

3. Results and Discussion

For a proper discussion and comparison of theoretical results, it is important to have a clear picture of the experimental data. We thus collect, in Table 1, the measured absorption maxima wavelengths for each dye; notice that, for L0 and D5, the spectra recorded in different solvents are available, thus giving us the possibility of investigating the solvatochromic effects.

A meaningful comparison of the calculated excitation energies with the experimental absorption maxima wavelengths requires inclusion of solvation effects and the possible deprotonation of the terminal cyanoacrylic acid[51] to be taken into account because, as is apparent, both effects induce consistent shifts (up to ca. 0.3 eV) in the measured excitation energies. Athough, usually, bulk solvent effects are efficiently included by resorting to a continuum model, like the conductor-like polarizable continuum model (C-PCM) based on the COSMO solvation model,[44,52,53] the explicit solvent−solute interactions (i.e., hydrogen-bonding), which become prominent in protic solvents, are partly missed in this approach. The explicit solvation of the moieties, which are more liable to give direct interactions with the solvent, generally provides a practical strategy to reproduce the main solvatochromic shifts. Furthermore, additional uncertainties in comparing computed and measured data arise from the fact that the computed vertical excitation energies (the difference between the energy of the excited state and that of the ground state at the optimized ground-state geometry, without zero-point energy corrections) do not have an actual experimental correspondence. Even if it is taken as an approximation to the position of the maximum of the absorption band, sizable discrepancies (0.1−0.15 eV) between the vertical calculated excitation energy and the maximum peak position have been computed.[54–56]

In the following, after addressing the problem of the calibration of the TDDFT methodology against high-level ab initio results in the gas phase, we shall discuss, in more detail, the protonation/deprotonation and the solvation effects, trying to reproduce the solvathocromic shifts by explicit solvation of the cyanoacrylate group.

3.1. Benchmarking on the Gas-Phase Results. Table 2 reports the computed transition energies in the gas phase for the lowest excited state of the dyes under investigation. As proposed by Peach et al.,[57] a direct way to quantify the extent of charge-transfer character of an electronic transition is to compute the spatial overlap between the occupied and unoccupied molecular orbitals involved in the excitation. Because

TABLE 2: Computed Excitation Energies (in eV) for the Lowest Excited State of D4, L0, D5, C217, and JK2. The Standard 6-31G* Basis Has Been Used for the TDDFT, CASSCF, and PC-NEVPT2 Calculations, Whereas the cc-pVDZ and cc-pVTZ Basis Sets Have Been Used for the Coupled Cluster Ones[d]

		TDDFT			Wave function methods			
dye	Λ	B3LYP[a]	MPW1K	CAM-B3LYP	EOM-CCSD	PC-NEVPT2[b]	RI-CC2[c]	CASSCF[b]
D4	0.52	3.10	3.46	3.48	3.53	3.64	3.16	4.24
L0	0.51	2.99	3.40	3.45	3.59	3.49	3.16	4.26
D5	0.47	2.23	2.70	2.97			2.72	
C217	0.38	1.96	2.50	2.64			2.50	
JK2	0.35	1.99	2.60	2.78			2.68	

[a] The B3LYP excitation energies with the 6-31+G* basis set are 2.91 (L0) and 2.19 eV (D5). [b] CAS(10/13). [c] The RI-CC2 calculated excitation energies with the cc-pVTZ basis set are 3.06 (L0), 3.07 (D4), and 2.61 eV (D5). [d] For each dye, the value of the spatial overlap between the HOMO and LUMO (B3LYP/6-31G* in vacuo), Λ, is also reported.

the lowest excited state of these push−pull dyes is essentially described by the HOMO → LUMO excitation, here, we get an approximate estimation of the degree of CT simply as the spatial overlap between the HOMO and LUMO moduli:

$$\Lambda = \int |\varphi_{\mathrm{HOMO}}(r)||\varphi_{\mathrm{LUMO}}(r)|dr$$

Let us start focusing the discussion on the smallest dyes, L0 and D4 (Figure 1), for which we performed high-level EOM-CCSD and PC-NEVPT2 calculations. The joint use of multiconfigurational and monoconfigurational wave function based methods, such as MRPT2 and coupled cluster, is an important diagnostic test because it allow us to evaluate the possible multiconfigurational character of the ground-state wave function (static correlation). Concerning the NEVPT2 calculations, it is important to remark that a crucial point for obtaining accurate excitation energies in a CASSCF/PT2 scheme, where the excitation energy is obtained as the difference between the excited-state energy and that of the ground state, is to have a balanced treatment of correlation effects in the two states. Therefore, particularly for such large aromatic systems, where only a reduced π space can be selected as active (14 active orbitals at most in the current implementation),[30] the choice of the active orbitals requires particular care and systematic tests. A preliminary evaluation on the use of various-sized active spaces has been, therefore, carried out, although, here, we shall just discuss the results attained with the larger CAS(10/13) space. Note that, for the smaller L0 molecule, we also performed calculations with a CAS(10/14), obtaining almost the same excitation energies reported in Table 2 (i.e., 4.25/4.26 and 3.50/3.49 eV at CASSCF and PC-NEVPT2 levels, respectively).

The ground-state CASSCF wave functions present a clear single reference nature, with the closed-shell Hartree−Fock determinant accounting for 86% (L0) and 84% (D4); other residual minor contributions arise from the single HOMO−LUMO transition and additional doubly excited configurations. Also, the excited-state wave functions have a well-defined nature, being principally dominated (about 76% for L0 and 74% for D4) by the single HOMO−LUMO excitation. Therefore, any problem related to the multireference nature of the ground-state wave functions can be reasonably excluded.

By looking at Table 2, it is quite clear that all the wave function-based methods provide similar excitation energies for L0 and D4, within 0.15 eV, although relevant differences are computed for the absolute excitation energy values.

The highest EOM-CCSD and PC-NEVPT2 levels of theory yield comparable excitation energies for both dyes, in the range of 3.49−3.64 eV. We further notice that closer results for L0 and D4 are obtained at the EOM-CCSD (3.59−3.53 eV for L0 and D4, respectively) rather than at the PC-NEVPT2 (3.49−3.64) level. Considering that, for the two systems, we obtain a similar single-reference ground state, the slightly larger variability of PC-NEVPT2 results mainly reflects the limits of the chosen active space, which introduces additional differences in the description of dynamic correlation. Indeed, at the CASSCF level, the excitation energies of the two dyes, although substantially overestimated, are almost coincident (4.26 and 4.24 eV for L0 and D4, respectively).

Interestingly, RI-CC2 values are noticeably too low compared to the higher-level EOM-CCSD results, with a difference of about 0.4 eV with the same cc-pVDZ basis; such discrepancies are, however, in line with those computed by Schreiber et al. in their recent benchmark study,[58] suggesting that CC2 values do not necessarily constitute a benchmark for DFT results. A further decrement of ca. 0.1 eV in the excitation energy is attained at the RI-CC2 level if the larger cc-pVTZ basis set is employed. Such a large discrepancy between the RI-CC2 and EOM-CCSD values clearly reveals a problematic description of the excited states, further attested by the computed values of the D1 diagnostic[59] at both RI-CC2 (0.1071 (L0) and 0.1127 (D4)) and EOM-CCSD (0.0856 (L0) and 0.0881 (D4)) levels. This suggests that strong orbital relaxation effects related to the CT phenomenon, rather than a multireference character of the ground-state wave function, could play a crucial role in the description of these systems. Unfortunately, higher-order coupled-cluster approaches, for example, CC3 or CCSD(T), which would allow us to provide a clearer picture of the expansion convergence, are not feasible for these realistic systems.

Turning to the TDDFT results for L0 and D4, the B3LYP x-c functional provides quite underestimated excitation energies for both dyes compared to our EOM-CCSD and PC-NEVPT2 benchmark results, predicting the lowest excited state at 2.99 (L0) and 3.10 eV (D4). Remarkably, a description in excellent agreement with the high-level ab initio results is attained by using the MPW1K and CAM-B3LYP functionals.

For the larger D5, C217, and JK2 dyes, one can reasonably extend the previous considerations on D4 and L0 because the investigated molecules have in common the triphenylamine and the cyanoacrylic acid as donor and acceptor moieties and only differ by an increasing conjugation across the spacer.

Considering the underestimation of excitation energies computed at the CC2 level discussed above and assuming that CC2 results should not be strongly affected by the increasing degree of CT, the computed data for D5, C217, and JK2 reported in Table 2 seem thus to indicate a progressive deterioration of the performance of the conventional hybrid functionals as Λ increases. Indeed, the B3LYP and the MPW1K x-c functionals tend, albeit to a different extent, to give too low excitation energies. On the other hand, in line with previous findings[57,60]

TABLE 3: Experimental Absorption Maxima and Computed Excitation Energies of the Lowest Excited State (eV) for the Protonated Dyes in vacuo and in Ethanol Solution; the Calculated Oscillator Strengths Are Also Reported

	MPW1K				B3LYP				exptl
	vacuum		solvent		vacuum		solvent		
dye	E_{exc}	f	E_{exc}	f	E_{exc}	f	E_{exc}	f	E_{exc}
D4	3.46	1.119	3.17	1.250	3.10	0.953	2.81	1.053	3.18
L0	3.40	0.980	3.16	1.075	2.99	0.796	2.72	0.886	3.21−3.32
D5	2.70	1.608	2.48	1.673	2.23	1.105	2.00	1.201	2.62−2.90
C217	2.50	1.810	2.32	1.924	1.96	0.933	1.74	1.065	2.25
JK2	2.60	1.444	2.45	1.549	1.99	0.668	1.82	0.767	2.84

TABLE 4: Experimental Absorption Maxima (eV) and Computed Excitation Energies (eV) of the Lowest Excited State for the Protonated and Deprotonated Dyes in Solvent; the Calculated Oscillator Strengths Are Also Reported

	MPW1K				B3LYP				exptl
	protonated		deprotonated		protonated		deprotonated		
dye	E_{exc}	f	E_{exc}	f	E_{exc}	f	E_{exc}	f	E_{exc}
D4	3.17	1.250	3.51	1.139	2.81	1.053	3.07	0.935	3.18
L0	3.15	1.075	3.46	0.661	2.73	0.886	2.89	0.469	3.21−3.32
D5	2.48	1.673	2.86	1.740	2.00	1.201	2.38	1.129	2.62−2.90
C217	2.32	1.924	2.67	2.148	1.74	1.065	2.15	1.543	2.25
JK2	2.45	1.549	2.81	1.714	1.82	0.767	2.26	0.880	2.84

as well as with the results of similar LC-TDDFT approaches,[61–65] CAM-B3LYP seems to provide the most stable and reliable results, predicting excitation energies very close to the highest-level ab initio results for D4 and L0 and always above the RI-CC2 values (by ca. 0.2−0.3 eV) for all the investigated dyes. We notice aside that, in light of these results, the good performance of the B3LYP or PBE0 functionals for the extended D102 and D149 indoline dyes[66–68] appears intriguing, suggesting that factors different from the electronic structure, for example, explicit solute−solvent interactions, might be responsible for those results.

Finally, as shown by the B3LYP excitation energies for L0 (2.91 eV) and D5 (2.19 eV) computed with the 6-31+G* basis and reported as a footnote in Table 2, the inclusion of a diffuse function does not significantly affect the results, yielding a negligible (<0.1 eV) lowering in the excitation energy.

3.2. Comparison with Experiment. As stated above, the comparison between theoretical results and experimental data, recorded in the condensed phase, imposes the use of effective solvation models and a careful examination of the possible chemical and physical phenomena taking place in solution. To simulate these effects, we resort to conventional TDDFT functionals, for which continuum solvation models are implemented in our version of Gaussian03.[38] We thus employ the MPW1K for subsequent investigations, which, based on the benchmark discussed above, is a reliable and computationally inexpensive approach for this class of push−pull dyes. For the sake of comparison, we also report B3LYP results.

In Table 3, we report the results for the protonated dyes in the gas phase and solution, whereas the effect of dye protonation/deprotonation in solution is analyzed in Table 4. To have a more coherent comparison, we present in both tables homogeneous results obtained in ethanol solution. We also performed additional calculations in different solvents (chloroform, acetonitrile), in order to better compare with the experimental conditions.

As shown in Table 3 and in Figure 2, where a scheme of the MO energy levels of the protonated and deprotonated C217 is reported, going from the gas phase to ethanol (chloroform) solution, a decrease of the HOMO−LUMO energy gap is observed with a consequent red shift of the lowest excitation energy, mainly described by the HOMO → LUMO excitation. Such a red shift, regardless of the x-c functional employed, is in the range of 0.15−0.30 eV and basically arises from the stabilization of the virtual orbitals in solution; in other terms, the charge-separated excited state is stabilized by the electrostatic interaction with the solvent.

In line with our previous results,[51] deprotonation of the cyanoacrylic moiety leads to a substantial blue shift of the lowest excitation energy; see Table 4. Here, we further notice that the effect of the deprotonation of the cyanoacrylic acid is more sensitive to the computational level as well as to the CT extent. The blue shifts computed in solution upon deprotonation with MPW1K go from 0.30 to 0.41 eV as the CT increases, whereas B3LYP tends to give lower blue shifts for the dyes with moderate CT and higher values for JK2 and C217. Moreover, as shown in Figure 2 for the C217 case with the MPW1K functional, deprotonation produces a sizable destabilization of the LUMO, clearly more pronounced in the nonpolar chloroform solvent, that reduces the electron-acceptor capability of the cyanoacrylic group.

Having established solvation and protonation/deprotonation effects, we are now able to compare our calculated results with available experimental data. For L0 and D5, the comparison with experimental data is straightforward because the protonation state for these two dyes was assigned experimentally.[36] For the deprotonated L0 and D5, we compute transition energies of 3.45 and 2.86 eV, in excellent agreement with the corresponding experimental data on the deprotonated dyes of 3.32 and 2.90 eV, respectively. Also, for the protonated D5 dye, we calculate a transition energy of 2.48 eV, to be compared to the corresponding 2.62 eV experimental absorption maximum.

It is also interesting in this stage to compare calculated and experimental data for the deprotonated dyes in ethanol and acetonitrile solutions. Our calculated results are almost insensitive to the change of solvent, providing a 0.01 eV red shift going from ethanol to acetonitrile: for L0 and D5, the computed excitation energies for the deprotonated species in MeCN (EtOH) are 3.45 (3.46) and 2.85 (2.86) eV, respectively. Because the considered solvents do not have too different dielectric constants (35.69 for acetonitrile and 24.85 for ethanol), a similar response is provided by the C-PCM calculations. A slightly larger blue shift (0.06 eV) is computed for C217: the MPW1K excitation energies for the deprotonated species are 2.67 and 2.73 eV in ethanol and in chloroform ($\varepsilon = 4.71$), respectively.

As shown in Table 1, experimentally, a ca. 0.1 eV blue shift is observed on going from ethanol to acetonitrile, but, as discussed above, this difference is not captured by the calculated results. One could expect that direct solute−solvent interactions, especially hydrogen-bonding, take place between the deprotonated cyanoacrylic group and the protic ethanol/methanol solvents; therefore, a partial protonation via hydrogen bonding might explain the observed slight red shift of the excitation energies retrieved experimentally. To model such explicit solute−solvent interactions, we performed additional calculations on the prototype D5 dye, adding two water molecules solvating the deprotonated cyanoacrylic group. The optimized geometry, obtained also in this case in the gas phase to better gauge the explicit solvent effect compared to data in Tables 3 and 4, is reported in Figure 3. The rather short computed O−H bond lengths ($O_1-H_{11} = 1.77$ Å and $O_2-H_{21} = 1.80$ Å) clearly indicate a strong hydrogen-bonding interaction between the

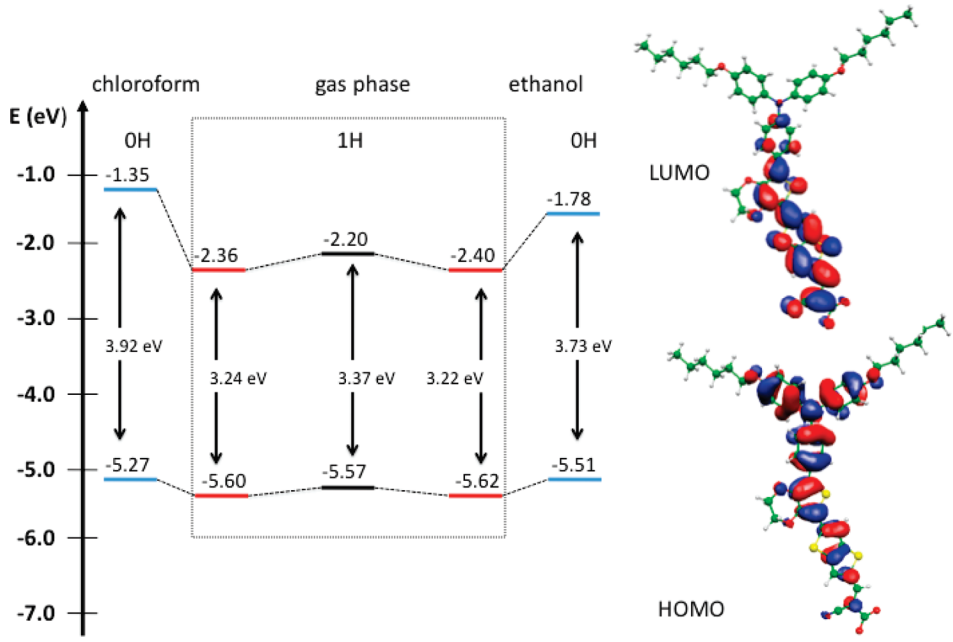

Figure 2. Scheme of the HOMO and LUMO energy levels (MPW1K/6-31G*) of the protonated (1H) and deprotonated (0H) C217 in vacuo, in ethanol (right), and in chloroform (left). The isodensity surfaces of the HOMO and LUMO in ethanol (deprotonated dye) are also plotted.

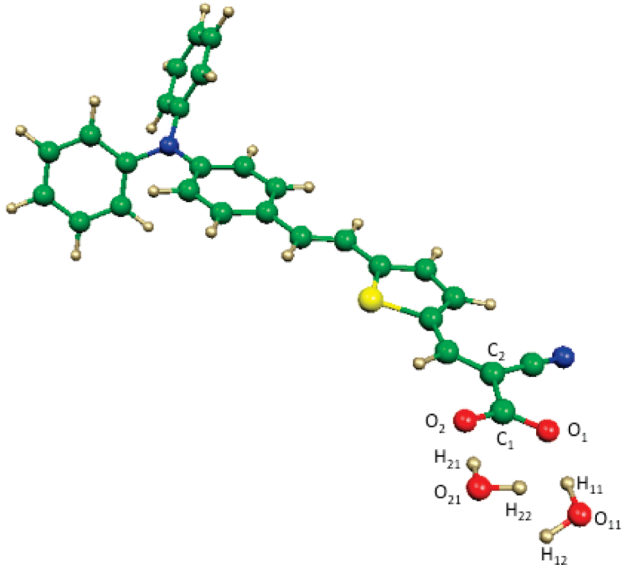

Figure 3. B3LYP/6-31G* optimized geometry of the deprotonated D5−2H_2O adduct.

cyanoacrylate group and the water molecules. A small reduction of the $O_2C_1O_1$ angle is also computed with respect to the optimized deprotonated molecule alone: upon addition of the two solvent molecules, it passes from 132.6° to 128.5°. The partial protonation via hydrogen bonding is also accompanied by a slight shortening of the C_1C_2 bond: 1.60 Å in the deprotonated D5 against 1.53 Å in the deprotonated D5−2H_2O adduct. Finally, we notice that the two H_2O molecules do not lie in the π plane of the molecule, being the H_{22} and H_{12} atoms, respectively, 17° and −36° out of the COO^- plane (Figure 3).

For the deprotonated D5−2H_2O adduct, the MPW1K lowest excitation energy is computed in ethanol solution at 2.81 eV, further improving the agreement with the corresponding experimental data in ethanol (2.81 eV), to be compared to the calculated excitation energy for the bare deprotonated dye of 2.86 eV. The slight red shift (0.05 eV) nicely compares with the experimental solvatochromic shift, confirming the effect of partial hydrogen bonding by protic solvents.

For D4 and JK2, a clear assignment of the protonation state is not available experimentally, but based on the effect of protic solvents discussed above, we expect experimental data in ethanol to be somehow intermediate between those calculated for protonated and deprotonated species. For D4, we calculate values of 3.17−3.51 eV for protonated/deprotonated species, which compare favorably with the 3.18 eV experimental absorption maximum. Similarly, for JK2, we calculate 2.45−2.81 excitation energies for protonated/deprotonated species, in good agreement with the experimental value of 2.84 eV. Despite the fact that the calculated values are within the expected range of accuracy, considering all the effects discussed above, it seems, however, that the MPW1K functional slightly overestimates/underestimates the electronic transitions for the L0-D4/JK2 dyes, in line with the results obtained in the gas phase (Table 2). This is most likely due to the static description of the Hatree-Fock exchange with the interelectronic distance, which introduces a rigid system-independent shift of the transition energies,[20] similar to that observed with the BH&H functional.[69] Finally, for C217, we believe it is rather safe to compare experimental data in chloroform with calculated data for the protonated dye because deprotonation is quite unlikely to take place in such an apolar solvent. In this case, the calculated 2.32 eV vertical excitation nicely compares with the 2.25 eV absorption maximum.

For the sake of completeness, we conclude our analysis discussing the choice of the geometry optimization level by comparing, in Table 5, the excitation energies (MPW1K/6-31G*) obtained from differently optimized ground-state geometries. We note that the B3LYP and the PBE0 functionals yield very similar excitation energies, within 0.03 eV, whereas the MPW1K method tends to give higher (up to ca. 0.1 eV) values. Moreover, the B3LYP and PBE0 results are in better agreement with the energies obtained from the ab initio MP2 geometries than the MPW1K ones, thus confirming the accuracy of the widely used B3LYP/6-31G* method for the ground-state geometry optimizations.

TABLE 5: Comparison of the Excitation Energies (eV) of the Lowest Excited State of L0 and D5 Obtained at the MPW1K/6-31G* Level from Ground-State Geometries (Both Protonated and Deprotonated) Optimized in the Gas Phase Using a 6-31G* Basis Set and Different Methodologies

		MPW1K/6-31G*		
		gas phase	solvent	
system	geometry optimization method	protonated	protonated	deprotonated
L0	B3LYP	3.40	3.15	3.46
	MPW1K	3.46	3.21	3.52
	PBE0	3.40	3.14	3.46
	MP2	3.35	3.10	3.40
D5	B3LYP	2.70	2.47	2.86
	MPW1K	2.79	2.58	2.98
	PBE0	2.72	2.50	2.88
	MP2	2.73	2.53	2.85

4. Concluding Remarks

We have performed an extensive theoretical investigation employing state-of-the-art TDDFT methodologies and highly correlated wave function methods on a significant sample of organic dyes effectively employed in dye-sensitized solar cells (L0, D4, D5, C217, and JK2), with the aim of assessing the accuracy of TDDFT and setting up an accurate and efficient computational protocol to simulate their optical properties. The benchmark calculations, carried out in the gas phase on the L0 and D4 dyes, have shown, as previously observed, that the CAM-B3LYP approach is the more accurate TDDFT method among those tested here. We also proved that the MPW1K x-c functional, incorporating a fixed amount of Hartree−Fock exchange (ca. 42%), represents a practical and efficient choice to describe the excited state of this class of organic dyes, even if its performances tend to slightly deteriorate as the degree of charge transfer increases.

We have thus explored the effect of solvation and protonation/deprotonation of the terminal cyanoacrylic group on the dyes' optical properties. We found a remarkable agreement between the calculated excitation energies and the experimental absorption maxima of those dyes whose protonation/deprotonation state in solution was experimentally assessed. On the other hand, when there was no experimental evidence of protonation/deprotonation of the dye, the comparison between the calculated and the measured absorption spectra was not straightforward. Indeed, the use of a continuum solvent model, in which the explicit solute−solvent interactions are neglected, did not account for the solvatochromic shifts experimentally observed, delivering almost coincident excitation energies in different protic and aprotic solvents with not too different dielectric constants. By explicitly solvating by two water molecules the cyanoacrylate group of the prototypical D5 dye, we have shown the importance, in protic solvents, of taking into account the partial protonation through hydrogen bonding of the dissociated carboxylic function. Our model calculation on the D5−$2H_2O$ adduct almost quantitatively reproduced the experimental 0.1 eV red shift of the lowest excited state going from acetonitrile to ethanol solution.

In conclusion, our study has demonstrated that a proper TDDFT formulation can successfully describe the excited-state properties of a series of organic dye sensitizers for solar cell applications, yielding results of comparable quality to high-level correlated ab initio calculations. Our study has also stressed the importance of properly comparing calculated results with experimental measurements, taking into account solvation and dye protonation/deprotonation issues.

Overall, our investigation paves the way to the reliable computational design and predictive screening of organic dyes sensitizers, even before their synthesis, in analogy to what already has been achieved for transition-metal complexes.

Acknowledgment. M.P., E.M., and F.D.A. thank Fondazione Istituto Italiano di Tecnologia (IIT), Project SEED 2009 (HELYOS), for financial support. M.G. acknowledges support by the Swiss National Science Foundation.

Note Added after ASAP Publication. This paper was erroneously published without final corrections on the Web March 29, 2010. The corrected version was reposted April 1, 2010.

References and Notes

(1) O'Regan, B.; Grätzel, M. *Nature* **1991**, *353*, 737.
(2) Grätzel, M. *J. Photochem. Photobiol., A* **2004**, *164*, 3–14.
(3) Nazeeruddin, M. K.; De Angelis, F.; Fantacci, S.; Selloni, A.; Viscardi, G.; Liska, P.; Ito, S.; Takeru, B.; Grätzel, M. *J. Am. Chem. Soc.* **2005**, *127*, 16835–16847.
(4) Ito, S.; Zakeeruddin, S. M.; Humphry-Baker, R.; Liska, P.; Charvet, R.; Comte, P.; Nazeeruddin, M. K.; Péchy, P.; Takata, M.; Miura, H.; Uchida, S.; Grätzel, M. *Adv. Mater.* **2006**, *18*, 1202–1205.
(5) Ito, S.; Miura, H.; Uchida, S.; Takata, M.; Sumioka, K.; Liska, P.; Comte, P.; Pechy, P.; Grätzel, M. *Chem. Commun.* **2008**, 5194–5196.
(6) Zhang, G.; Bala, H.; Cheng, Y.; Shi, D.; Lv, X.; Yu, Q.; Wang, P. *Chem. Commun.* **2009**, 2198–2200.
(7) Kim, S.; Lee, J. K.; Kang, S. O.; Ko, J.; Yum, J. H.; Fantacci, S.; De Angelis, F.; Di Censo, D.; Nazeeruddin, M. K.; Grätzel, M. *J. Am. Chem. Soc.* **2006**, *128*, 16701–16707.
(8) Horiuchi, T.; Miura, H.; Sumioka, K.; Uchida, S. *J. Am. Chem. Soc.* **2004**, *126*, 12218–12219.
(9) Fantacci, S.; De Angelis, F.; Selloni, A. *J. Am. Chem. Soc.* **2003**, *125*, 4381–4387.
(10) Fantacci, S.; De Angelis, F.; Sgamellotti, A.; Marrone, A.; Re, N. *J. Am. Chem. Soc.* **2005**, *127*, 14144–14145.
(11) Abbotto, A.; Barolo, C.; Bellotto, L.; De Angelis, F.; Grätzel, M.; Manfredi, N.; Marinzi, C.; Fantacci, S.; Yum, J.; Nazeeruddin, M. K. *Chem. Commun.* **2008**, 5318–20.
(12) Vlček, A. J.; Zaìliš, S. *Coord. Chem. Rev.* **2007**, *251*, 258–287.
(13) De Angelis, F.; Fantacci, S.; Selloni, A. *Nanotechnology* **2008**, *19*, 424002.
(14) Grätzel, M. *Acc. Chem. Res.* **2009**, *42*, 1788–1798.
(15) Barone, V.; Polimeno, A. *Chem. Soc. Rev.* **2007**, *36*, 1724–1731.
(16) Jacquemin, D.; Perpète, E. A.; Ciofini, I.; Adamo, C. *Acc. Chem. Res.* **2009**, *42*, 326–334.
(17) Dreuw, A.; Weisman, J. L.; Head-Gordon, M. *J. Chem. Phys.* **2003**, *119*, 2943–2946.
(18) Tozer, D. J. *J. Chem. Phys.* **2003**, *119*, 12697–12699.
(19) Jacquemin, D.; Perpete, E. A.; Scuseria, G. E.; Ciofini, I.; Adamo, C. *J. Chem. Theory Comput.* **2008**, *4*, 123–135.
(20) Magyar, R. J.; Tretiak, S. *J. Chem. Theory Comput.* **2007**, *3*, 976–987.
(21) Tawada, Y.; Tsuneda, T.; Yanagisawa, S.; Yanai, T.; Hirao, K. *J. Chem. Phys.* **2004**, *120*, 8425–8433.
(22) Kamiya, M.; Sekino, H.; Tsuneda, T.; Hirao, K. *J. Chem. Phys.* **2005**, *122*, 234111.
(23) Iikura, H.; Tsuneda, T.; Yanai, T.; Hirao, K. *J. Chem. Phys.* **2001**, *115*, 3540–3544.
(24) Yanai, T.; Tew, D. P.; Handy, N. C. *Chem. Phys. Lett.* **2004**, *393*, 51–57.
(25) Rohrdanz, M. A.; Martins, K. M.; Herbert, J. M. *J. Chem. Phys.* **2009**, *130*, 054112.
(26) Rohrdanz, M. A.; Herbert, J. M. *J. Chem. Phys.* **2008**, *129*, 034107.
(27) Lange, A. W.; Rohrdanz, M. A.; Herbert, J. M. *J. Phys. Chem. B* **2008**, *112*, 6304–6308.
(28) Werner, H.-J.; Knowles, P. J. *J. Chem. Phys.* **1988**, *89*, 5803–5814.
(29) Andersson, K.; Malmqvist, P. A.; Roos, B. O.; Sadlej, A. J.; Wolinski, K. *J. Phys. Chem.* **1990**, *94*, 5483–5488.
(30) Angeli, C.; Pastore, M.; Cimiraglia, C. *Theor. Chem. Acc.* **2007**, *117*, 743–754.
(31) Stanton, J. F.; Bartlett, R. J. *J. Chem. Phys.* **1993**, *98*, 7029–7039.
(32) Rhee, Y. M.; Head-Gordon, M. *J. Phys. Chem. A* **2007**, *111*, 5314–26.
(33) Hagberg, D. P.; Edvinsson, T.; Marinado, T.; Boschloo, G.; Hagfeldt, A.; Sun, L. C. *Chem. Commun.* **2006**, 2245–2247.

(34) Hagberg, D. P.; Yum, J.-H.; Lee, H.; De Angelis, F.; Marinado, T.; Karlsson, K. M.; Humphry-Baker, R.; Sun, L.; Hagfeldt, A.; Grätzel, M.; Nazeeruddin, M. K. *J. Am. Chem. Soc.* **2008**, *130*, 6259–6266.

(35) Kitamura, T.; Ikeda, M.; Shigaki, K.; Inoue, T.; Anderson, N. A.; Ai, X.; Lian, T.; Yanagida, S. *Chem. Mater.* **2004**, *16*, 1806–1812.

(36) Hagberg, D. P.; Marinado, T.; Karlsson, K. M.; Nonomura, K.; Qin, P.; Boschloo, G.; Brinck, T.; Hagfeldt, A.; Sun, L. *J. Org. Chem.* **2007**, *72*, 9550–9556.

(37) Horiuchi, T.; Miura, H.; Uchida, S. *Chem. Commun.* **2003**, 3036–3037.

(38) Frisch, M. J.; Trucks, G. W.; Schlegel, H. B.; Scuseria, G. E.; Robb, M. A.; Cheeseman, J. R.; Montgomery, J. A., Jr.; Vreven, T.; Kudin, K. N.; Burant, J. C.; Millam, J. M.; Iyengar, S. S.; Tomasi, J.; Barone, V.; Mennucci, B.; Cossi, M.; Scalmani, G.; Rega, N.; Petersson, G. A.; Nakatsuji, H.; Hada, M.; Ehara, M.; Toyota, K.; Fukuda, R.; Hasegawa, J.; Ishida, M.; Nakajima, T.; Honda, Y.; Kitao, O.; Nakai, H.; Klene, M.; Li, X.; Knox, J. E.; Hratchian, H. P.; Cross, J. B.; Adamo, C.; Jaramillo, J.; Gomperts, R.; Stratmann, R. E.; Yazyev, O.; Austin, A. J.; Cammi, R.; Pomelli, C.; Ochterski, J. W.; Ayala, P. Y.; Morokuma, K.; Voth, G. A.; Salvador, P.; Dannenberg, J. J.; Zakrzewski, V. G.; Dapprich, S.; Daniels, A. D.; Strain, M. C.; Farkas, O.; Malick, D. K.; Rabuck, A. D.; Raghavachari, K.; Foresman, J. B.; Ortiz, J. V.; Cui, Q.; Baboul, A. G.; Clifford, S.; Cioslowski, J.; Stefanov, B. B.; Liu, G.; Liashenko, A.; Piskorz, P.; Komaromi, I.; Martin, R. L.; Fox, D. J.; Keith, T.; Al-Laham, M. A.; Peng, C. Y.; Nanayakkara, A.; Challacombe, M.; Gill, P. M. W.; Johnson, B.; Chen, W.; Wong, M. W.; Gonzalez, C.; Pople, J. A. *Gaussian 03*, revision B05; Gaussian Inc.: Wallingford, CT, 2003.

(39) Becke, A. D. *J. Chem. Phys.* **1993**, *98*, 1372–1377.

(40) Lynch, B. J.; Fast, P. L.; Harris, M.; Truhlar, D. G. *J. Phys. Chem. A* **2000**, *104*, 4811.

(41) Adamo, C.; Barone, V. *J. Chem. Phys.* **1999**, *110*, 6158–6170.

(42) Petit, L.; Maldivi, P.; Adamo, C. *J. Chem. Theory Comput.* **2005**, *1*, 953–962.

(43) DALTON, a molecular electronic structure program, release 2.0 (2005); see http://www.kjemi.uio.no/software/dalton/dalton.html.

(44) Cossi, M.; Barone, V. *J. Chem. Phys.* **2001**, *115*, 4708–4717.

(45) Christiansen, O.; Koch, H.; Jørgensen, P. *Chem. Phys. Lett.* **1995**, *243*, 409–418.

(46) Werner, H.-J.; Knowles, P. J.; Lindh, R.; Manby, F. R.; Schütz, M.; Celani, P.; Korona, T.; Rauhut, G.; Amos, R. D.; Bernhardsson, A.; Berning, A.; Cooper, D. L.; Deegan, M. J. O.; Dobbyn, A. J.; Eckert, F.; Hampel, C.; Hetzer, G.; Lloyd, A. W.; McNicholas, S. J.; Meyer, W.; Mura, M. E.; Nicklass, A.; Palmieri, P.; Pitzer, R.; Schumann, U. H.; Stoll, A. J. S.; Tarroni, R.; Thorsteinsson, T. *MOLPRO, a package of ab initio programs*, version 2006.1.

(47) Dunning, J. T. H. *J. Chem. Phys.* **1989**, *90*, 1007–1023.

(48) Alhrichs, R.; et al. *TURBOMOLE*, v. 5.10; University of Karlsruhe: Karlsruhe, Germany.

(49) Hättig, C.; Weigend, F. *J. Chem. Phys.* **2000**, *113*, 5154.

(50) Hättig, C.; Hellweg, A.; Köhn, A. *Phys. Chem. Chem. Phys.* **2006**, *8*, 1159–1169.

(51) Abbotto, A.; Manfredi, N.; Marinzi, C.; De Angelis, F.; Mosconi, E.; Yum, J.; Xianxi, Z.; Nazeeruddin, M. K.; Grätzel, M. *Energy Environ. Sci.* **2009**, *2*, 1094.

(52) Klamt, A.; Schüürmann, G. *J. Chem. Soc., Perkin Trans. 2* **1993**, 799–805.

(53) Cossi, M.; Rega, N.; Scalmani, G.; Barone, V. *J. Comput. Chem.* **2003**, *24*, 669–681.

(54) Dierksen, M.; Grimme, S. *J. Chem. Phys.* **2004**, *120*, 3544–3554.

(55) Santoro, F.; Improta, R.; Lami, A.; Bloino, J.; Barone, V. *J. Chem. Phys.* **2007**, *126*, 1–13.

(56) De Angelis, F.; Santoro, F.; Nazeruddin, M. K.; Barone, V. *J. Phys. Chem. B* **2008**, *112*, 13181–13183.

(57) Peach, M. J. G.; Benfield, P.; Helgaker, T.; Tozer, D. J. *J. Chem. Phys.* **2008**, *128*, 044118.

(58) Schreiber, M.; Silva-Junior, M. R.; Sauer, S. P. A.; Thiel, W. *J. Chem. Phys.* **2008**, *128*, 134110.

(59) Janssen, C. L.; Nielsen, I. M. B. *Chem. Phys. Lett.* **1998**, *290*, 423–430.

(60) Cai, Z.-L.; Crossley, M. J.; Reimers, J. R.; Kobayashi, R.; Amos, R. D. *J. Phys. Chem. B* **2006**, *110*, 15624–15632.

(61) Wong, B. M.; Cordaro, J. G. *J. Chem. Phys.* **2008**, *129*, 214703.

(62) Stein, T.; Kronik, L.; Baer, R. *J. Chem. Phys.* **2009**, *131*, 244119.

(63) Jacquemin, D.; Perpète, E. A.; Scalmani, G.; Frisch, M. J.; Kobayashi, R. *J. Chem. Phys.* **2007**, *128*, 144105.

(64) Jacquemin, D.; Perpete, E. A.; Vydrov, O. A.; Scuseria, G. E.; Adamo, C. *J. Chem. Phys.* **2007**, *127*, 094102.

(65) Wong, B. M.; Piacenza, M.; Sala, F. D. *Phys. Chem. Chem. Phys.* **2009**, *11*, 4498.

(66) Jose, R.; Kumar, A.; Thavasi, V.; Fujihara, K.; Uchida, S.; Ramakrishna, S. *Appl. Phys. Lett.* **2008**, *93*, 023125.

(67) Pastore, M.; De Angelis, F. *ACS Nano* **2010**, *4*, 556–562.

(68) Le Bahers, T.; Pauporté, T.; Scalmani, G.; Adamo, C.; Ciofini, I. *Phys. Chem. Chem. Phys.* **2009**, *11*, 11276–11284.

(69) Preat, J.; Michaux, C.; Jacquemin, D.; Perpete, E. A. *J. Phys. Chem. C* **2009**, *113*, 16821–16833.

JP100713R